Convection in White Dwarf Stars

Kevin J. P. Luecke

Table of Contents

1. Introduction

White dwarfs are some of the simplest stars. Because of their simplicity, they can be studied to learn fundamental facts about the universe. By studying them, we can learn about their progenitors, and 97% of stars end their lives a white dwarfs. They can also be used to find the age of the galactic disc (Winget et al. (1987)). These determinations, however,

rely on the accuracy of our models of white dwarfs. In white dwarf science and the field of Astrophysics in general, one of the most prevalent, and least understood phenomena is convection. The reason for this uncertainty is the non-local nature of convection. One could argue that the beginning of modern science, (certainly classical physics) came with Newton and the development of calculus. Calculus is the system we use to describe change, and has been widely applied across the sciences. However, this technique, while incredibly useful, cannot describe non-local phenomena, or situations where any point can be effected by far off points. Convection is just such a situation. Because you can't break these problems down to a simple, local approximation, we have no analytical tools to solve them. These kind of problems went largely unsolved until recently.

With the advent of the computer came the hope of computing the effects of convective regions directly from first principals. Unfortunately, to compute the effects exactly you need an unattainable amount of computational power. By making some assumptions and simplifications, however, you can bring the problem into a regime which is computable by modern, massively parallel computers. This kind of simulation has been achieved in many stars, most notably the sun (Stein and Nordlund (1998)). To confirm the accuracy of these solar simulations data from luminosity variations along the surface can be used. For other stars, however, no such spatial resolution is possible, so some other effect of convection must be measured. Fortunately, pulsations in certain classes of white dwarfs interact with convection giving us just such an effect. By fitting models of stars with these two interacting phenomena to data from real stars, we can learn more about convection in the physical regime of white dwarfs, as well as about the white dwarfs themselves.

2. Turbulent energy transport

Turbulent energy transport, or convection occurs in most stars, including our sun. It even occurs in planets like the earth. Understanding convection better can help us understand all the stars and even possibly earth weather. To be able to parametrize this phenomena, we have to first understand why it happens.

2.1. Condition for Convection

In order for convection to occur, when a fluid element gets displaced, it must keep moving rather than return to its original position. To understand under what conditions this happens, we use the Lagrangian formulation of perturbation theory, and track the displaced

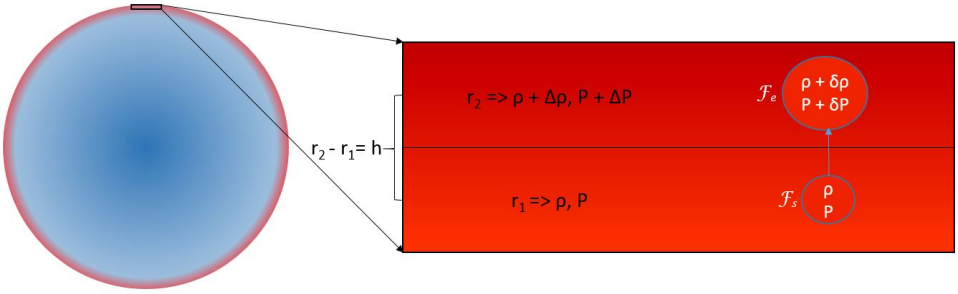

Fig. 1.— Lagrangian Description of Condition for Convection: This image is not to scale. In reality the slice of the stellar atmosphere we are talking about is a tiny sliver that takes up much less of the star than the rectangle pictured indicates.

fluid element. This is illustrated in Figure 1.

Let our fluid element be moved from r_1 to r_2. As these are two different radii, they have slightly different values of P and ρ. At r_1 we define the following values for the pressure and density:

$$P_{r_1} = P$$

$$\rho_{r_1} = \rho$$

and at r_2 we define

$$P_{r_2} = P + \Delta P$$

$$\rho_{r_2} = \rho + \Delta\rho.$$

Our fluid element $\mathcal{F}$ will start with the same properties as the rest of the fluid at r_1, namely:

$$P_{\mathcal{F}_s} = P$$

$$\rho_{\mathcal{F}_s} = \rho$$

As it rises, however, its *pressure* will change to remain in equilibrium with its surroundings. For this step we make the adiabatic assumption, namely that this step happens fast enough that there is not enough time for the fluid element to lose or gain energy or particles, so the entropy of the fluid element remains constant. For the pressure to equalize with the surroundings, the volume and therefor density of the fluid element has to change. This sets the fluid element $\mathcal{F}$ to the new values of:

$$P_{\mathcal{F}_e} = P + \delta P$$

$$\rho_{\mathcal{F}_e} = \rho + \delta\rho.$$

From pressure equilibrium at its new position we know:

$$P_{\mathcal{F}_e} = P_{r_2}$$

$$P + \delta P = P + \Delta P$$

$$\delta P = \Delta P.$$

For the element to continue to rise (as it must if the region is convective), it has to be lighter than its surroundings, i.e., have a lower density, so:

$$\rho_{\mathcal{F}_e} < \rho_{r_2}$$

$$\rho + \delta\rho < \rho + \Delta\rho$$

$$\delta\rho < \Delta\rho.$$

If, on the other hand:

$$\delta\rho = \Delta\rho$$

$\mathcal{F}$ will stay at r_2, and if:

$$\delta\rho > \Delta\rho$$

$\mathcal{F}$ will fall back to r_1.

So now we just have to determine $\Delta\rho$ and $\delta\rho$ in terms of the properties of the star. As we are looking at a very small fraction of the star's radius, we can just do a first order approximation in this region, meaning:

$$\rho_{r_2} = \rho_{r_1} + h\frac{d\rho}{dr}$$

$$\rho + \Delta\rho = \rho + h\frac{d\rho}{dr}$$

$$\Delta\rho = h\frac{d\rho}{dr}.$$

Similarly:

$$\Delta P = h\frac{dP}{dr}.$$

To find $\delta\rho$, we have to know how ρ changes as a function of P, with the entropy held fixed. This is known as the equation of state. In general, we can write the equation of state in this form:

$$\rho = \rho(P, S).$$

Here ρ is a function of pressure and entropy, however, in our fluid element, the entropy does not have time to change so:

$$\rho_{\mathcal{F}_e} = \rho(P_{r_2}, S_{r_1}) = \rho(P + \Delta P, S)$$

Expanding around $\rho(P, S)$ we have

$$\rho_{\mathcal{F}_e} = \rho(P, S) + \Delta P \left(\frac{\partial \rho}{\partial P}\right)_S + \Delta S \left(\frac{\partial \rho}{\partial S}\right)_P,$$

and since the entropy is constant ($\Delta S = 0$), this yields

$$\rho_{\mathcal{F}_e} = \rho(P, S) + \Delta P \left(\frac{\partial \rho}{\partial P}\right)_S$$

$$\rho + \delta\rho = \rho + h\frac{dP}{dr}\left(\frac{\partial \rho}{\partial P}\right)_S$$

$$\delta\rho = h\frac{dP}{dr}\left(\frac{\partial \rho}{\partial P}\right)_S.$$

So the condition for convection to occur is:

$$\delta\rho < \Delta\rho$$

$$h\frac{dP}{dr}\left(\frac{\partial \rho}{\partial P}\right)_S < h\frac{d\rho}{dr}$$

$$\frac{dP}{dr}\left(\frac{\partial \rho}{\partial P}\right)_S < \frac{d\rho}{dr}.$$

The $\frac{dP}{dr}$ and $\frac{d\rho}{dr}$ terms are the changes in pressure and density respectively as we get farther out in the star. The pressure and density decrease from the center to the surface, so we can say

$$\frac{dP}{dr} < 0$$

$$\frac{d\rho}{dr} < 0$$

This means I can rearrange the inequality as given below:

$$\left(\frac{\partial \rho}{\partial P}\right)_S > \frac{\left(\frac{d\rho}{dr}\right)}{\left(\frac{dP}{dr}\right)} = \frac{d\rho}{dP}.$$

So in order for convection to occur, the local change in density with pressure in a region of the star has to be less than the adiabatic change in density with pressure. It is important to note that if we were to do a similar derivation for a fluid element displaced downwards towards the center of the star, that continued to sink, we would obtain the same result.

2.2. Mixing Length Theory

From the derivation above, we can conclude that convection does occur, and indeed it occurs somewhere in most stars. However, at this point our ability to interpret convection analytically ends. When these displaced fluid elements are lighter than the surrounding fluid, they speed up and continue to rise. This acceleration continues throughout the region of the star where the condition I derived above remains true. This makes it very hard to figure out what actually happens in these regions. If fluid elements can slam through a region changing the local conditions abruptly, it is hard to rely on any assumptions about local stability that lie at the heart of calculus.

Even following just one fluid element and keeping the rest fixed can lead to problems. If the fluid element keeps accelerating, minor differences in the density or pressure of the fluid through which it's moving can deflect or slow it, breaking it up unpredictably. Because of this, convection remains a largely unsolved problem today and one of the largest sources of uncertainty in stellar modeling (Montgomery (2005)).

Currently, the most commonly used approximation of convection is known as Mixing Length Theory. This method is only an order of magnitude approximation, and is used because it is easy to compute rather than because of any faith in its accuracy. As Kippenhahn says, "we do not believe it [mixing-length theory] to be sufficient, but it does provide at least a simple method for treating convection locally at any given point of a star." (Kippenhahn et al. (2013)). Basically, mixing-length theory assumes that convection happens over a certain length l_m (the "mixing length") and from there derives an equation for the energy flux through that section of the star. With this, most other properties of the star important to stellar evolution can be determined.

However, the correct value for l_m is not readily apparent. The normal *ad hoc* assumption is that the mixing length is some parameter α, which is of order 1, times the local pressure scale height, i.e.,

$$l_m = \alpha\, H_P,$$

where

$$H_P = -\frac{P}{dP/dr}.$$

This parameter α varies widely between different types of stars, which drastically reduces its predictive power. Fortunately with the power of the TACC (Texas Advanced Computing Center) and other super computers, a more complete treatment of this problem can be attained.

2.3. Antares

In order to better define the size and properties of the convection region of white dwarfs, I have attempted to simulate this convective region of the star. Hydrodynamic simulations take an Eulerian approach to fluid dynamics, breaking up the convective region into a grid of points each with their own values for ρ, P, T, and many other physical properties of matter. This simulation continuously updates these physical properties for each grid point after short time intervals based on the properties of the points around them. To figure out how to update each grid-point, the simulation relies on tables of measured equation of state relationships. This process of updating the grid-points relies only on basic principals of physics, so it's reliable, but computationally expensive. Getting it to complete in a realistic time frame requires a lot of algorithm refinement and optimization that balances speed with accuracy. The program I have used for this simulation is the ANTARES program, developed at the University of Vienna to simulate the convective region of the sun. I created a program to visualize this output. A sample rendering is shown in Figure 2. This program has had great success when applied to the sun and A-Stars, and is now being applied to large, Jupiter-like planets (Muthsam et al. (1995); Kupka and Muthsam (2008)). However, in the case of white dwarfs, I have run into some difficulties that appear to be caused by extremely fast moving fluid elements.

There are two speeds that are important in this simulation, the speed of the fluid element, and the sound speed. The sound speed is important because it controls the speed at which thermal equilibrium is reached. If we picture the star as a set of discrete layers, each with its own pressure, density, and temperature, a fluid element passing through these layers spends a discrete amount of time in each

$$t_{r_n} = \frac{h}{v_{\mathcal{F}}}.$$

This is the amount of time that the particles have to bounce around on the edge and exchange energy before the fluid moves on to the next layer. When I derived the condition for convection, I made the adiabatic assumption, which means I assumed that the fluid I was tracking moved too fast to settle into thermal equilibrium in any one of these layers. This means fluid in the region should bee moving pretty fast. If the velocity of the fluid element is extremely fast, however, approaching or even surpassing the sound speed, it will travel through layers of the star without changing much at all. If it stays this fast for long, and travels through a enough layers, it will eventually be surrounded by fluid with a very different temperature and density.

Using a tool I created to read and interpret the output of ANTARES, I found fluid moving with velocity greater than twice the speed of sound. This speed seems to be making

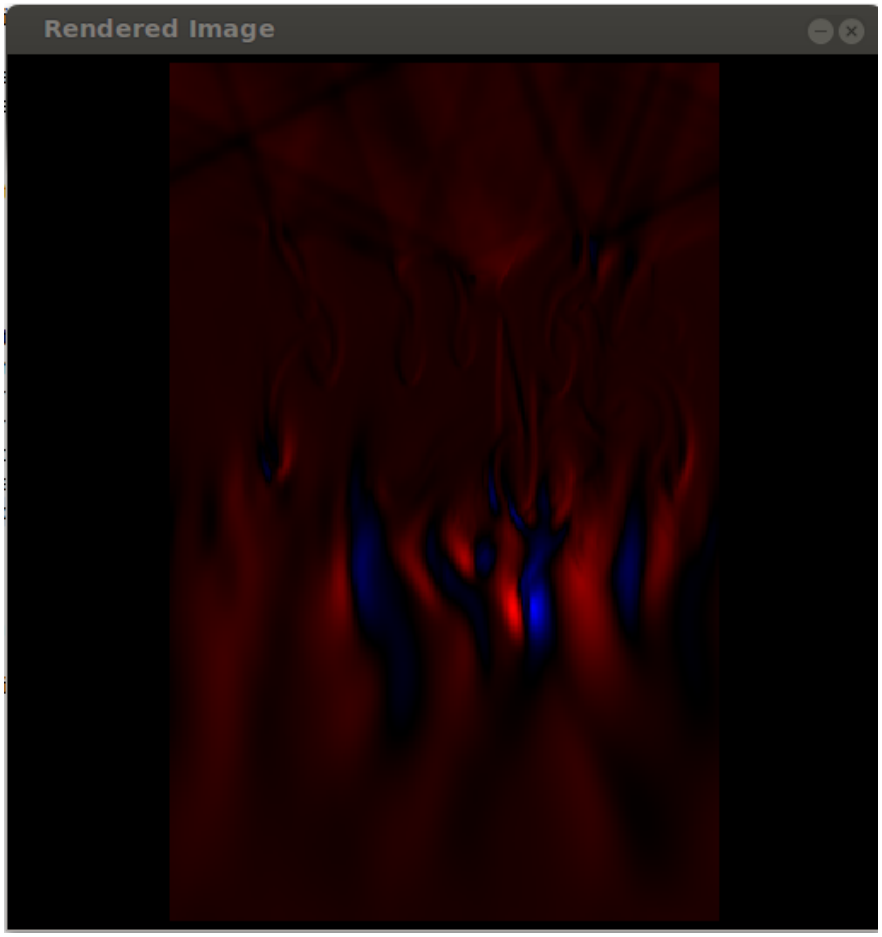

Fig. 2.— Radiative flux in one time-step of the program ANTARES.

adjacent grid points have wildly differing temperatures and densities. This pushes ANTARES equation of state lookups into regimes we haven't measured yet. Unable to resolve these gridpoints, the simulation ends before producing useful results. I have been unable to find a way to resolve this problem and leave it to future work.

3. Interaction Between Convection and Pulsations

Concurrently with the ANTARES project, I have been building on the work of my adviser Mike Montgomery. In his 2005 paper entitled "A New Technique for Probing Convection in Pulsating White Dwarf Stars", Montgomery builds on the work of Brickhill and that of Goldreich & Wu, in developing a technique to measure convection zone size by fitting observations (Brickhill (1992); Wu (2001); Montgomery (2005)). In this section I will follow

this derivation. This technique takes advantage of the extreme oscillations in the physical properties of the atmospheres of pulsating white dwarfs.

As part of their evolutionary cycle, white dwarfs with hydrogen atmospheres (DAs) enter what is known as the instability strip, where they can change in brightness by 10% in a matter of minutes, as pictured in Figure 4. These brightness variations are a result of harmonic oscillations in temperature and density throughout the star. These variations in brightness (or energy flux), then should be described by standard harmonic oscillations of a spherical object:

$$F = \sum_j Re[A_j e^{i(\omega_j t + \delta_j)} Y_{l_j,m_j}(\theta, \phi)].$$

Here the characteristic sinusoidal behavior of a wave is represented by $A_j e^{i(\omega_j t+\delta_j)}$, each of the j waves, has an amplitude A, a frequency ω, and a phase δ. The effects of the spherical structure of the star are taken into account through Lapace's spherical harmonic equations, $Y_{l,m}(\theta, \phi)$, where θ and ϕ are spherical coordinates, and l and m are integers such that $-l < m < l$. This fits our observations fairly well, however the light curves show additional nonlinear effects. These effects have long been attributed to convection (Brickhill (1992)). As a star pulsates, the fundamental physical parameters of the star (e.g., its temperature and density) change. When these parameters change, so does the size of its convective envelope.

Three facts about these stars make it possible to parametrize this constantly changing convection zone. First of all, the time it takes a convection zone to relax into stable state (convective turnover timescale) is much less than the time is takes a pulsation to complete a cycle. Secondly, the radial size of the convection zone is much smaller than the radial wavelength of a pulsation. This means at any given time we can assume the the convection zone on any section of the surface of the star is the same as a convection zone of a non-pulsating star in equilibrium at that temperature. Finally, as the convective envelope lies on the very outer edge of the star, we can assume that the energy flux underneath the convection zone strictly follows the equation above.

As a fluid becomes convective its method of energy transport changes, which can be thought of like a phase change. This means the energy flux leaving the star is the flux entering the convective region minus the energy it takes to "change the phase" of fluid elements from convective to non-convective:

$$F_{phot} = F_{base} - \tau_C \frac{dF_{phot}}{dt},$$

where τ_C is the convective turnover timescale and can be thought of as the heat capacity of the convection zone. The formula for the flux at the base is the standard model for white dwarfs mentioned earlier. Using mixing length theory, we can estimate the convective

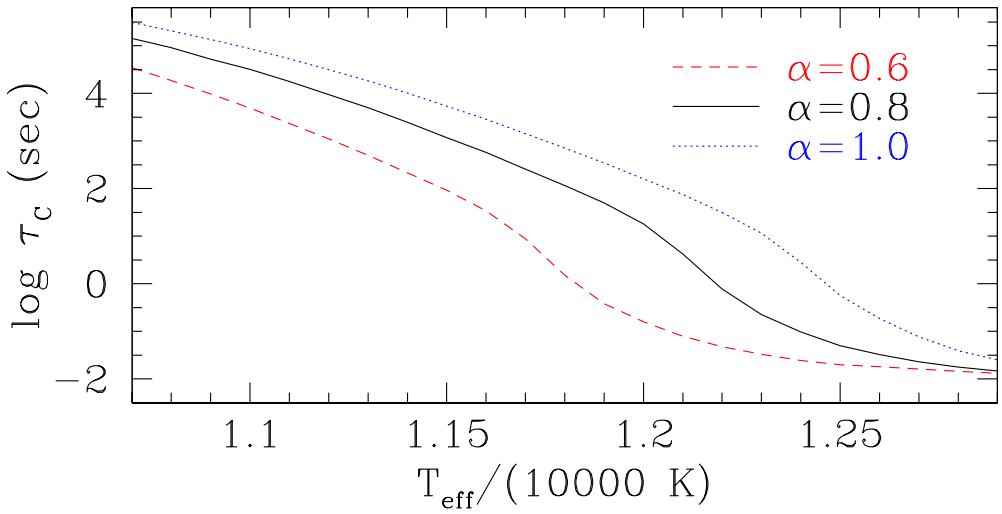

Fig. 3.— Value of the convective turnover timescale as a function of effective temperature as predicted by mixing length theory. A few different values of α that are appropriate for white dwarfs have been plotted.

timescale as a function of temperature. Even if you vary the mixing length parameter α, τ_C is fitted by a power of $T_{\rm eff}$. To see this more clearly we can plot $\log(\tau_C(T_{\rm eff}))$, and notice that it is nearly linear, with a negative slope (see Figure 3). From this we can approximate the convective timescale:

$$\tau_C(T_{\rm eff}) \approx \tau_0 \times \left(\frac{T_{\rm eff}}{T_{\rm eff,0}}\right)^{-N}$$

Here $T_{\rm eff,0}$ is the starting temperature, τ_0 is a constant depending on α, and N is a constant approximately between 90 and 95 in DAs. This supports the theory that τ_C is strongly dependent on T, and the convection zone strongly effects the energy flux at the photosphere (F_{phot}).

Using this model as the basis for a fitting program, Montgomery has been able to reproduce the light curves of simple stars with extreme accuracy. However, this program is not able to fit all of the parameters quickly enough to be useful on complex stars. To fix this problem, I have expanded the program to take advantage of massively parallel hardware on personal computers as well as that available to University of Texas students through the Texas Advanced Computing Center (TACC).

3.1. Lcfit_theta and GAMA

The program Montgomery wrote fit effects of convection zones on light curves is called Lcfit_theta. This program solves the following ordinary differential equation (ODE), reproduced in full:

$$F_{phot} = -\left[\tau_0 \times \left(\frac{T_{\rm eff}}{T_{\rm eff,0}}\right)^{-N}\right]\frac{dF_{phot}}{dt} + \sum_j Re[A_j e^{i(\omega_j t+\delta_j)} Y_{l_j,m_j}(\theta,\phi)]$$

This equation has the free parameters of the convection zone, τ_0 and N, as well as A_j, ω_j, δ_j, l_j, and m_j for each mode of oscillation. Additionally, there is the final free parameter which measures the orientation of the axis of pulsation relative to earth (known as the inclination angle θ_I). This final parameter comes into play when we attempt to create the light curve predicted by this model. Fortunately, using the simple approximation of the star as a spherical oscillator we can find each ω_j, and we get a good starting guess for each δ_j and A_j. Using mixing length theory, we can also find a good starting guess for N (namely 90-95 for DAs) and τ_0.

Up to this point, Lcfit_theta has only been fast enough to refine the initial guesses for N, τ_0, θ_I, A, and δ for each pulsation frequency. So users have to put in their own guesses for l and m of each frequency. This strategy is tractable if you are fitting a star with a small number of frequencies; however, for stars with many frequencies, this creates too many possibilities to test. Not trying all the possible combinations calls into question the values of the parameters we do fit, which is a shame as this technique is one of the only ways we can probe l and m values of the pulsation modes. Better determining both the convection zone size and spherical harmonics of the pulsation modes will help us improve our understanding of the interiors of these stars.

This leaves two possible areas of improvement. First of all, we can make this fit as it is implemented now run faster. To do this, we take advantage of the fact that, to accurately model the flux we see, we need to break up the surface of the star into a grid of points small enough that we can assume they have uniform temperature. Since we are solving the same equation on all of these grid points, we can speed up the simulation by solving this equation for all the grid points concurrently on massively parallel architecture like multicore computers and GPUs.

The second way to improve this fitting program is to programmatically fit the values of l and m. One way to do this is to run the fit on a wide range of l and m values concurrently on a machine with a large array of CPUs and/or GPUs. The TACC's newest resource, Stampede, has just such a heterogeneous architecture.

Designing a program to run efficiently on heterogeneous hardware with a variable number of CPUs and GPUs is by no means a solved problem. It is in fact a subject of ongoing research, and one group at the University of Texas is working in collaboration with the University of Minho on a system for just this purpose (Mariano (2012)). Their system is named GAMA for the "GPU And Multi-core Aware" framework. This system provides memory and resource management systems that dynamically balance the workload between all available resources. Users simply write a kernel (part of the algorithm that gets run repeatedly) or two, if they need different implementations on the CPU and GPU, and a dice function that receives resource statistics from GAMA and divides its workload into a list of jobs for GAMA to schedule.

3.1.1. Description of GPU Implementation

To be compatible with GAMA, my implementation of the ordinary differential equation solver had to compile with NVIDIA's CUDA compiler. This required a complete rewrite of the part of the program I was targeting to the GPU, namely the solution to the ordinary differential equation.

To solve this part of the equation, I follow the same procedure as Montgomery. In order to evaluate the accuracy of the parameters chosen, we must employ our model of the star over the time it was observed, construct the light curve our model would create, and compare it to the observed light curve. First, we note that only the part of the stellar surface that faces us contributes to the light we receive in our telescopes. This part still has widely varying temperatures across it, however. To take this into consideration, we must break the surface into a grid fine enough that, within each section, the temperature doesn't vary significantly. Then, for each grid-point, we need to integrate over the ordinary differential equation from a starting point (chosen to be the beginning of the first run) through the end of the final run. To accomplish this I employed a library entitled "ODEInt" that was included in the BOOST C++ libraries at the end of 2012. This library includes an implementation of the Dormand-Prince method, which is a fifth order Runge-Kutta style integration method (Butcher (1996)). The problem we are solving is known as an initial value problem, for which all you know is an initial starting point and an expression to calculate the derivative of the function at any given point. To calculate the derivative of the flux from our section of the star, we need to first calculate the flux at the base of the convection zone. This means simply evaluating the expression:

$$\sum_j Re[A_j e^{i(\omega_j t+\delta_j)} Y_{l_j,m_j}(\theta,\phi)]$$

for our current values of A_j, δ_j, l_j, and m_j at the time (t) in question. The values for θ and ϕ are determined by the grid-point (k). Calculating this flux directly, each calculation performs surprisingly well. I also implemented a solution that involves calculating a grid of solutions for the value of $F_{base}(k,t)$ and interpolating between them when solving the ODE. A simple linear interpolation scheme produces a maximum speed-up of approximately 10% over the integration with minor loss of accuracy (four times as inaccurate, but still of order 10^{-5}). Any higher order interpolation schemes take longer than simply calculating the flux directly. From this value we can compute the flux at the surface by applying the formula derived above.

When we have integrated up to a time for which our light curve has a data point, we have to sum up the contributions from each grid-point to get our simulated point. This process is complicated by an effect known as limb darkening. This effect is due to the curvature of the stellar surface we are simulating. Because of this curvature less flux from the edges of the area we are simulating contributes than from the center. Limb darkening effects can be parametrized as:

$$F_{obs} = \sum_k \mu(k, F_{phot}(k,t)) \times F_{phot}(k,t)$$

To solve account for this effect, I read in a grid of computed values for $\mu(k, F_{phot})$ and interpolate between them over the two dimensional space. Unfortunately, this grid is to course for a bi-linear interpolation to give accurate results. I therefor employed the cubic spline approach, following numerical recipies as was done in the CPU implementation.

3.2. Wu's Approximation

Although this multithreaded implementation increases the speed of lcfit_theta dramatically, it still can take a long time to search all values of l and m. In order to reduce the number of complicated fits needed, I implemented a simpler approximation that can find the values of l and m that are likely to be a best fit.

I took this formulation from the work of Wu in 2001 (Wu (2001)). This approximation takes the same form as the model of the flux at the base of the convection zone:

$$F = \sum_j Re[A_j e^{i(\omega_j t + \delta_j)} Y_{l_j,m_j}(\theta,\phi)]$$

It simply changes apparent amplitude (A) and phase (δ) of each witnessed mode to approximate the effects of a convection zone of base size τ_0 according to:

$$A_{phot} = \frac{A_{fbase}}{\sqrt{1 + (\omega_{fbase}\tau_0)^2}}$$

$$\delta_{phot} = \delta_{fbase} - \arctan(\omega\tau_0)$$

To implement this, I still divide the surface into a grid, but for each point I simply calculate the flux at each timestep according to the above equations. I have also implemented this fitting method with GAMA, so it can take full advantage of all the the host computer's resources while it is running. As it does not require an integration, this technique runs orders of magnitude faster than the full integration.

Wu's method does not always find the same values as 'best fit' as the full integration, however, it does seem to find better fits for the same values of l and m. In order to test this, I have run both methods on a few stars simple enough to preform an exhaustive search with the full integration method. So far it Wu's method has identified all of the same of the values that the full integration has identified. While this does not prove that Wu's method will identify the "best fit" according to Montgomery's method, it does give us a technique for intelligently narrowing the set of l and m values that we calculate fully.

4. Targets and Data Acquisition

In order to test the accuracy of my implementation I have reproduced the results obtained by the linear version of lcfit_theta on the target G29-38. On top of that, however I have chosen a target that will test its capabilities, HS0507+0435.

4.1. HS0507

This target tests the limits of my program as it has many more oscillatory modes than the aforementioned stars, as well as a few closely spaced modes that require a few nights of data to resolve. This means it has a large set of parameters to fit, as well as a long time period to integrate over on each fit.

This star was the subject of a recent paper by Fu et al. (who refer to the star as HS0507+0434B) (Fu et al. (2013)). In this paper, Fu lists 18 independent frequencies as well as a number of other signals due to the nonlinearities in the light curve. Fu includes a set of "preliminary identification[s]" of the l and m values as well as a discussion of their constraints of these. Using lcfit_theta we can determine these values more reliably. Fu notes that in his runs he found variation in the excited pulsation frequencies, and that "More observational data and theoretical investigations are needed to explore the physical causes of those visibilities". Fu discussed data from runs starting in 2007 and 2009. I have worked

with people at the University of Texas, The Central Texas Astronomical Society, and Paul Chote of the to reclaim 36-inch telescope at McDonald Observatory to collect further data.

4.2. Instrumentation

I had a few problems setting up the 36-inch for science. We wanted to clone an experiment that was running on the 82-inch telescope at McDonald Observatory. The system started with a spare camera and acquisition computer from the 82-inch telescope. This equipment had been used to develop the 82-inch system, so it should have been fully functional, however, it hit a few snags on the 36 -inch. The first of these problems manifested itself as an unusually high level of static on every image we took. By systematically switching out components with their counterparts on the 82-inch telescope I was able to determine that the problem was with the camera itself. The broken component turned out to be a small chip that monitored temperature levels for the camera cooling system. Without this component, the camera was not able to sense its own temperature, so it would not cool. The noise we had seen was just thermal noise from the ambient room temperature. The mounting screws used were a bit too long and had penetrated just far enough into the camera to hit this component. Fortunately, this was a relatively inexpensive part, and we were able to order a replacement.

The second problem we encountered manifested as a series of bands that appeared across the image. This turned out to be a high frequency interference originating from the motor that controlled the stepping of the telescope when tracking. The signal was passing along the wire that transferred the analog image to the control box. As the frequency was high we had to ground the control box to the telescope, by mounting it on the telescope directly.

Later that year, Argos, the camera used for out parent experiment on the 82-inch telescope, broke. That meant the camera we had been using on the 36-inch, Raptor, had to be re-appropriated. Fortunately, a new camera was purchased to replace the broken one. As this camera was of a newer model, it did not work with the old acquisition software. In order to use it, I developed a new acquisition system that could control it. This software was fully capable of controlling the camera and running our experiment, however, it was not able to communicate with the GPS timing system we had previously used. Fortunately, we were able to adopt a system developed by Paul Chote that had a custom timing devices and had been tested on similar observations.

Using this system I was able to gather data on HS0507 in December 2012 and March 2013. Data from the December run is reproduced in Figures 4 and 5

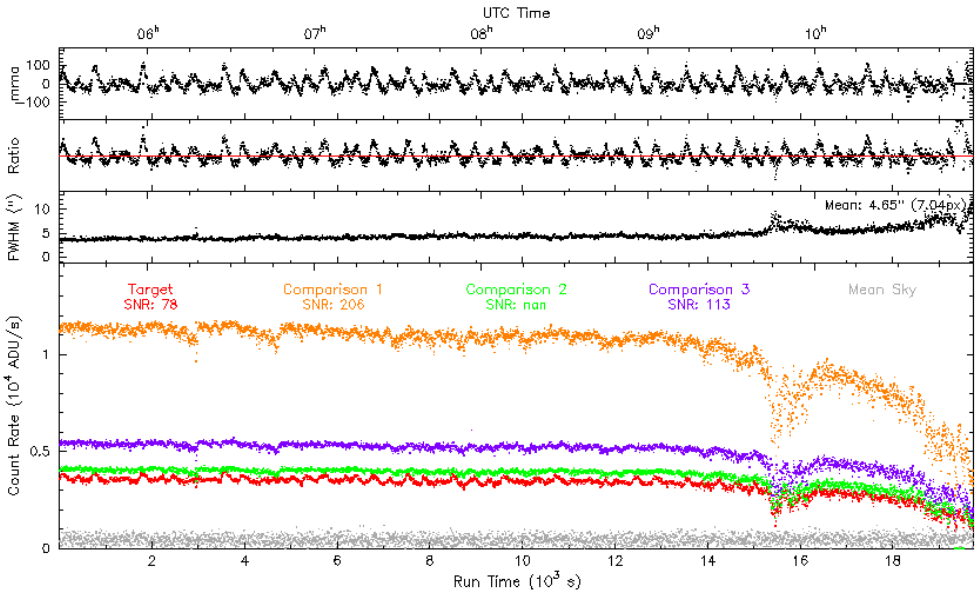

Fig. 4.— Observation of HS05057+0854 taken at the 36" telescope at McDonald Observatory on December 12^{th} 2012. The bottom graph is the measured values of the tracked stars. The top graph is the brightness of HS0507+0835 corrected for cloud cover and instrumental deficiencies, measured in $\frac{1}{1000}$ths of its average brightness.

5. Results and Discussion

Using MAESTRO, WQED and Period04, I have reduced the data from the December run on HS0507. The Fourier Transform is displayed in Figure 5. From this data, I was able to find 10 frequencies as listed in Figure 6.

Using the parallel version of Lcfit_theta, I was able to find the best fit to these data as shown in figure 7. This solution, while the best, was not obviously unique. Other values of m can be substituted for most modes to produce results that are extremely similar. Examples of other fits found are displayed in figure 8 for comparison. This ambiguity is partially due to the enormous number of modes and the relatively short dataset. However, this does reveal a significant ambiguity in the l and m values of the modes found.

These best fits come from the set of all possibles values of l and m where $l <= 2$. Interestingly, all the best fits have l values of 1. Most likely, this is simply an artifact of the limitation of the data set, if it is real, however, it is also quite interesting. It could come from the fact that the modes I detected are the most obvious in the star, and therefore are l equals 1 modes. If this is the case, I would expect to find other, smaller l equals 2 modes with a longer dataset. The existence of more modes is supported by figure 5, which shows the

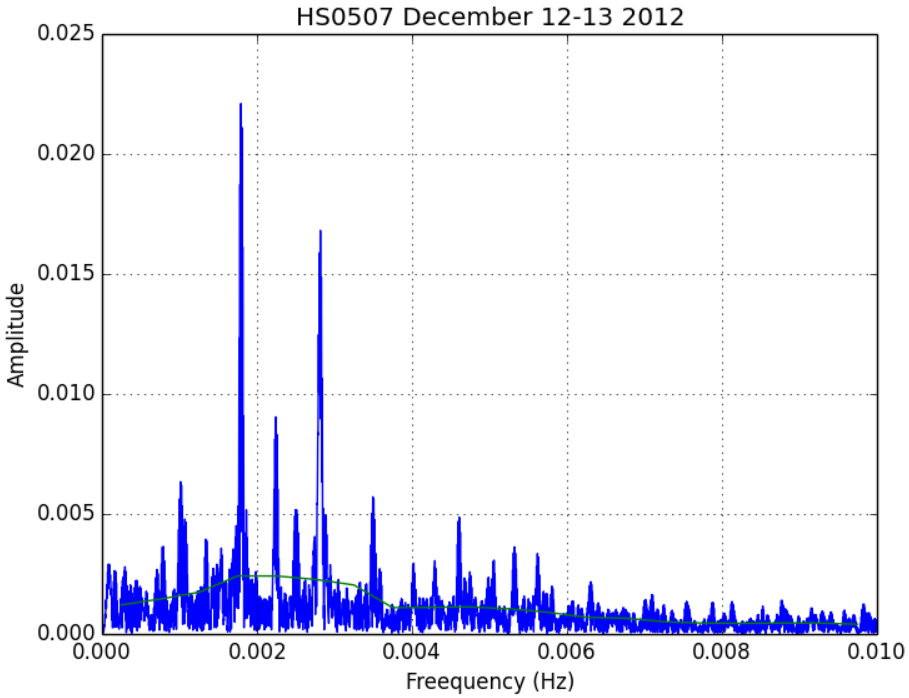

Fig. 5.— Fourier transform of observations in Figure 4 and the following night. observations were reduced separately combined to produce the ft shown

fourier transform of the data after removing all of the statistically significant modes. There is a good chance that some of these peaks are in fact real modes. This is also supported by the fact that Fu et al. found 18 independent modes when they looked at this star (Fu et al. (2013)).

Now that these calculations can take advantage of the full power of the Stampede super computer, we finally can actually run Montgomery's model on all the likely l and m values for each mode. This ability has exposed an ambiguity in the l and m values of the modes of the complex star HS0507. This result, is only preliminary because of th limitations of the dataset and more investigation needs to be done. However, Montgomery's model is most sensitive to the highest amplitude modes, so the addition of further, weaker signals is unlikely to produce enough of an effect to remove this result.

REFERENCES

Brickhill, A. (1992). The pulsations of zz ceti stars. v-the light curves. vi-the amplitude spectra. *Monthly Notices of the Royal Astronomical Society*, 259:519–535.

Butcher, J. (1996). A history of runge-kutta methods. *Applied numerical mathematics*, 20(3):247–260.

Fu, J.-N., Dolez, N., Vauclair, G., Machado, L. F., Kim, S.-L., Li, C., Chen, L., Alvarez, M., Su, J., Charpinet, S., et al. (2013). Asteroseismology of the zz ceti star hs 0507+ 0434b. *Monthly Notices of the Royal Astronomical Society*, 429(2):1585–1595.

Kippenhahn, R., Weigert, A., and Weiss, A. (2013). *Stellar structure and evolution*. Springer.

Kupka, F. and Muthsam, H. (2008). Analysing the contributions in moment equations of reynolds stress models of convection with numerical simulations. *Proceedings of the International Astronomical Union*, 252:463.

Mariano, A. M. M. (2012). *Scheduling (ir)regular applications on heterogeneous platforms*. PhD thesis, University of Minho, Department of Computer Science.

Montgomery, M. H. (2005). A new technique for probing convection in pulsating white dwarf stars. *The Astrophysical Journal*.

Muthsam, H., Göb, W., Kupka, F., Liebich, W., and Zöchling, J. (1995). A numerical study of compressible convection. *Astronomy and Astrophysics*, 293:127–141.

Stein, R. and Nordlund, Å. (1998). Simulations of solar granulation. i. general properties. *The Astrophysical Journal*, 499(2):914.

Winget, D., Hansen, C., Liebert, J., Van Horn, H., Fontaine, G., Nather, R., Kepler, S., and Lamb, D. (1987). An independent method for determining the age of the universe. *The Astrophysical Journal*, 315(2):L77–L81.

Wu, Y. (2001). Combination frequencies in the fourier spectra of white dwarfs. *Monthly Notices of the Royal Astronomical Society*, 323(1):248–256.

This preprint was prepared with the AAS LaTeX macros v5.2.

Name	Freq	Amp	Phase	Period
F1	0.001792	0.02051	0.947471	557.8832
F2	0.002817	0.017748	0.07364	354.9667
F3	0.002811	0.011923	0.154717	355.766
F4	0.002244	0.009242	0.248567	445.6455
F5	0.001013	0.006538	0.528501	987.1283
F6	0.002499	0.005684	0.224825	400.0861
F7	0.003506	0.005551	0.59494	285.2019
F8	0.001812	0.005338	0.061732	551.7976
F9	0.00461	0.004828	0.896444	216.9103
F10	0.001069	0.004752	0.328638	935.4779

Fig. 6.— Frequencies found in 36-inch December run on HS0507 using Period04

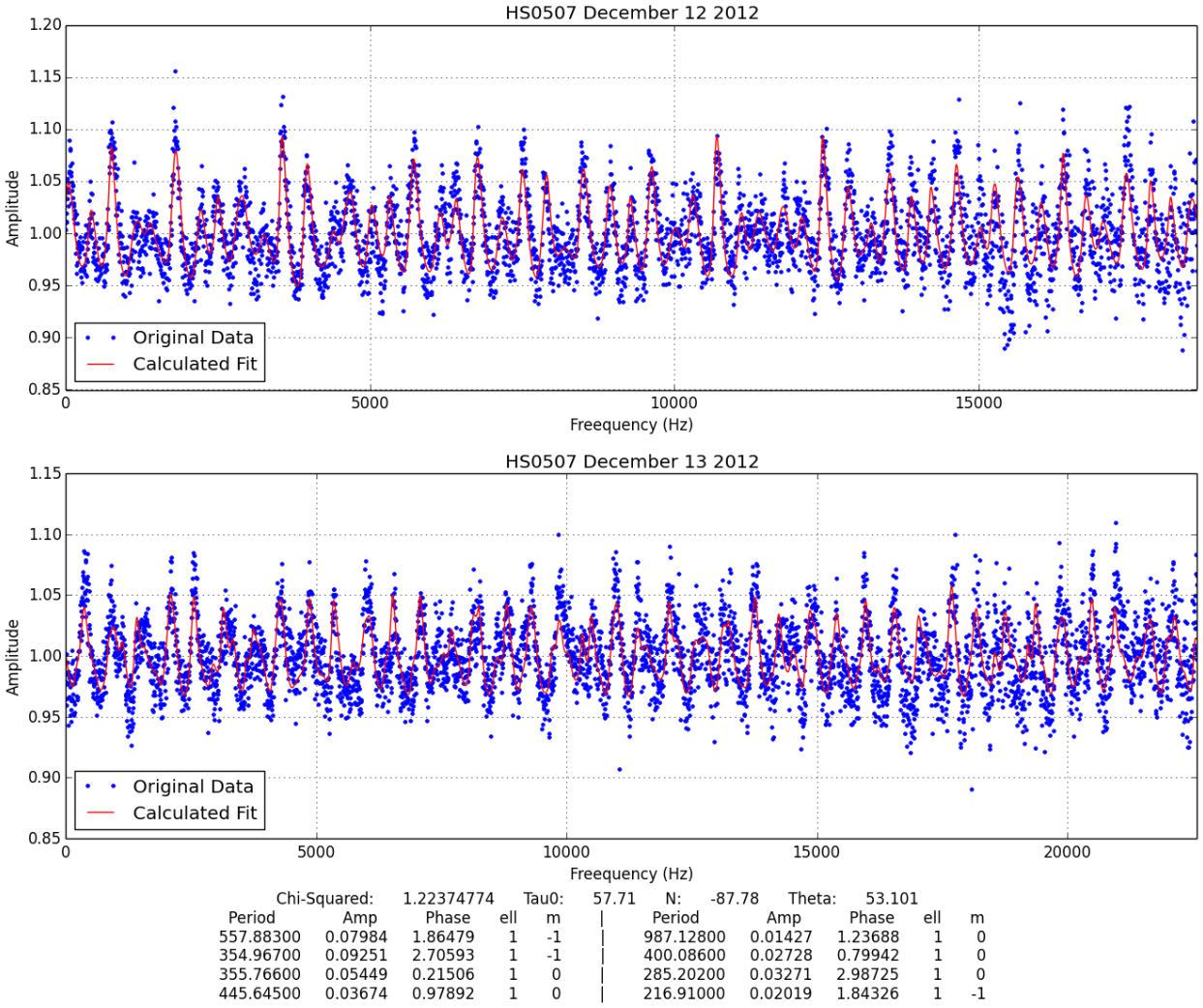

Chi-Squared: 1.22374774 Tau0: 57.71 N: -87.78 Theta: 53.101

Period	Amp	Phase	ell	m	Period	Amp	Phase	ell	m
557.88300	0.07984	1.86479	1	-1	987.12800	0.01427	1.23688	1	0
354.96700	0.09251	2.70593	1	-1	400.08600	0.02728	0.79942	1	0
355.76600	0.05449	0.21506	1	0	285.20200	0.03271	2.98725	1	0
445.64500	0.03674	0.97892	1	0	216.91000	0.02019	1.84326	1	-1

Fig. 7.— Data from December 12th and 13th 2012. Fit produced by Lcfit_theta

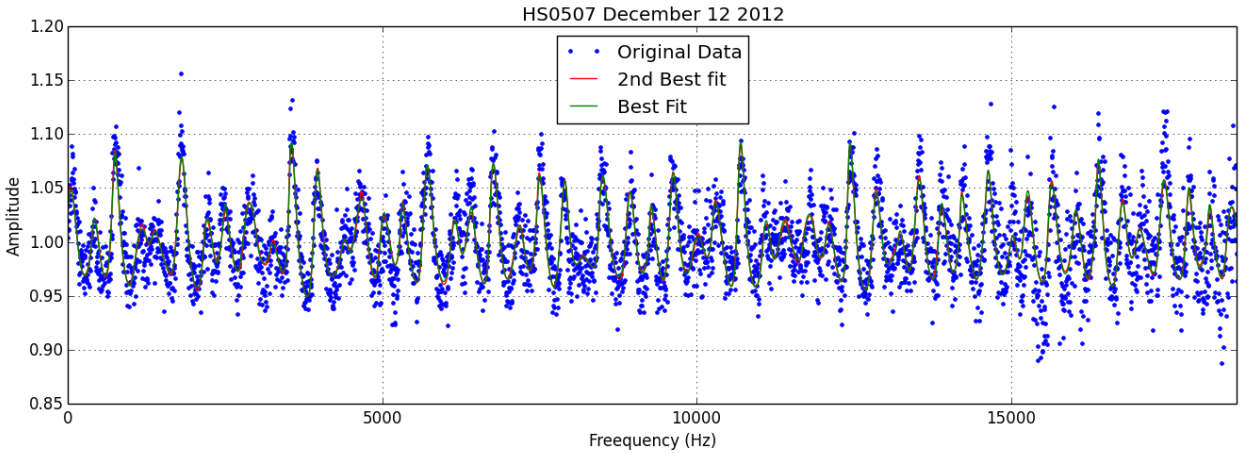

Chi-Squared: 1.22914361 Tau0: 51.66 N: -84.89 Theta: 55.655

Period	Amp	Phase	ell	m	Period	Amp	Phase	ell	m
557.88300	0.07429	1.81465	1	-1	987.12800	0.01562	1.34192	1	0
354.96700	0.08261	2.69039	1	-1	400.08600	0.02367	0.73551	1	1
355.76600	0.05383	0.14076	1	0	285.20200	0.03213	3.00946	1	0
445.64500	0.03639	0.96211	1	0	216.91000	0.01818	1.78059	1	-1

Fig. 8.— Comparison of best fit and second best fit. Data from December 12th. Fit produced by Lcfit_theta. Chi-Squared and fit values displayed is for the second best fit

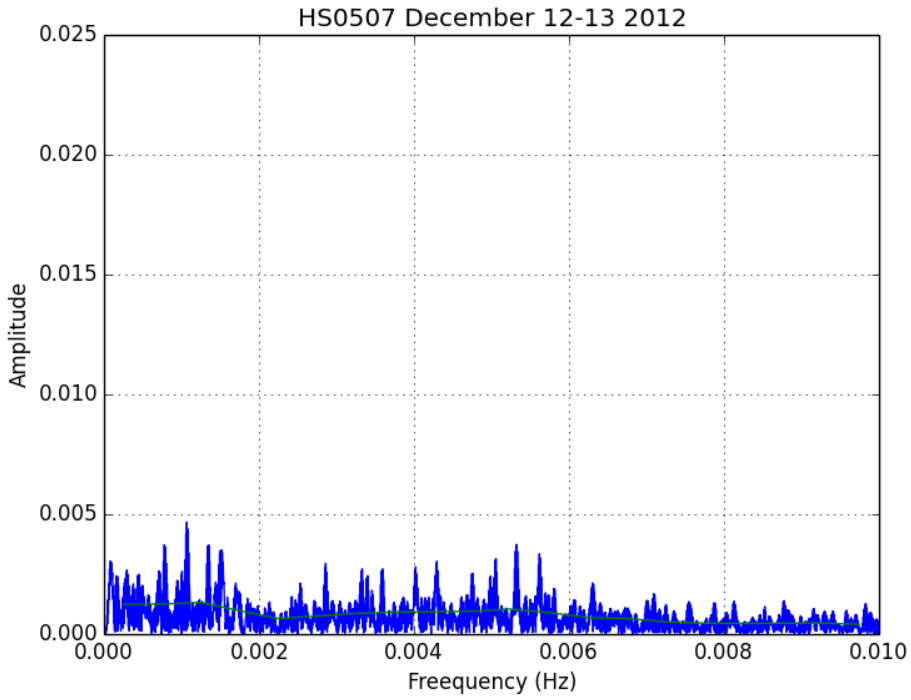

Fig. 9.— Figure 5 after removing identified frequencies